Published in final edited form as:
Cell Host Microbe. 2009 December 17; 6(6): 523–535. doi:10.1016/j.chom.2009.11.006.

Adenovirus Transport through a Direct Cytoplasmic Dynein-Hexon Interaction

K. Helen Bremner[a], **Julian Scherer**[a,*], **Julie Yi**[a,*], **Michael Vershinin**[b,*], **Steven P. Gross**[b], and **Richard B. Vallee**[a]

[a]Department of Pathology and Cell Biology, Columbia University, New York, NY 10032, U.S.A.

[b]Department of Developmental and Cell Biology, 2222 Nat. Sci. I, University of California-Irvine, Irvine, CA 92697, U.S.A.

SUMMARY

Early in infection, adenovirus travels to the nucleus as a naked capsid using the microtubule motor cytoplasmic dynein. This study was initiated to address how the virus recruits dynein, and to explore the role of dynein's diverse regulatory factors in virus transport. Cytoplasmic dynein, dynactin and NudE/NudEL, but not LIS1 or ZW10, colocalized with incoming, post-endosomal adenovirus particles. Dynein alone interacted in a pH-dependent manner with the adenovirus subunit hexon, which, in turn, interacted with recombinant dynein intermediate chain and light intermediate chain 1. Interference with dynactin function had no effect on dynein colocalization with adenovirus, but reduced virus run length. Expression of hexon or injection of anti-hexon antibody inhibited virus transport without affecting Golgi distribution. These results identify hexon as a direct receptor for cytoplasmic dynein, which recruits dynein for transport to the nucleus by a mechanism both novel and distinct from that for known physiological dynein cargo forms.

Keywords

Adenovirus; hexon; dynein; dynactin; microtubule; transport

INTRODUCTION

Many viruses travel long distances through the cytoplasm to reach the nucleus following cell entry. Diffusional spreading of viruses through the cytoplasm is severely limited, and the characteristics of motion of a number of viruses are instead consistent with transport by microtubule motors (Dohner et al., 2005). Recent evidence has implicated cytoplasmic dynein in the translocation of herpes simplex virus, adenovirus, African swine fever virus, rabies virus, and HIV to the nucleus (Alonso et al., 2001; Greber and Way, 2006; Jacob et al., 2000; Leopold

Corresponding author: Dr. Richard B. Vallee, Columbia University, College of Physicians and Surgeons, P&S 15-409, 630 West 168 Street, New York, NY 10032, USA, Phone: 212-342-0546, Fax: 212-305-5498, rv2025@columbia.edu.
*These authors contributed equally to this work.

Competing Financial Interests
The authors declare no competing financial interests.

et al., 2000; Sodeik et al., 1997; Suomalainen et al., 1999). How viruses recruit cytoplasmic dynein for their own transport is, however, poorly understood.

Adenovirus, a 90–100 nm diameter non-enveloped dsDNA virus, is a particularly attractive system for studying dynein-mediated transport. The capsid is very simple, consisting of just 14 polypeptides, and the infectious pathway is well characterized. Receptor-mediated endocytosis is followed by exit to the cytoplasm within 15 min, with loss of several capsid proteins (Cotten and Weber, 1995; Greber et al., 1996; Greber et al., 1993; Wiethoff et al., 2005). Further successive loss of capsid components occurs *en route* to the nucleus. Transport of the post-endosomal capsid along microtubules is bidirectional, and viruses accumulate at the centrosome and nuclear pores by 1 hr post-infection (p.i.) (Leopold et al., 2000; Suomalainen et al., 1999) when the 36 kb genome and associated proteins enter the nucleus (Trotman et al., 2001). Cytoplasmic dynein has been specifically implicated in adenovirus transport by the effects of anti-dynein antibody injection and overexpression of the dynactin subunit dynamitin. These treatments prevented virus from reaching the nucleus and, in the case of dynamitin, interfered with virus transport in live cell assays (Leopold et al., 2000; Suomalainen et al., 1999).

How the dynein complex is recruited to physiological forms of subcellular cargo is only partially understood, but even less is known about its recruitment by viruses. The dynein intermediate, light intermediate, and light chains (ICs, LICS, LCs) reside at the base of the dynein complex associated with the N-terminus of the dynein heavy chain (HC), where cargo binding is thought to occur. The ICs interact with another multi-subunit complex, dynactin (Karki and Holzbaur, 1995; Vaughan and Vallee, 1995), which links dynein to membrane vesicles and kinetochores directly or through the ZW10 complex (Burkhardt et al., 1997; Starr et al., 1998; Varma et al., 2006). Dynactin has also been implicated in motor processivity (King and Schroer, 2000; Ross et al., 2006). Several additional dynein regulatory proteins, including LIS1, NudE, NudEL, and NudC, have received attention for their role in nucleokinesis and brain developmental disease Of these, NudE and NudEL have also been implicated in dynein targeting to mitotic kinetochores and centrosomes (Guo et al., 2006; Stehman et al., 2007). A role for these factors in virus transport has not been examined.

Dynein and dynactin have been reported to interact with purified adenovirus, adeno-associated virus (Kelkar et al., 2006; Kelkar et al., 2004), and parvovirus (Suikkanen et al., 2003). Interactions with individual virus polypeptides have also been reported, but the relevance of these to virus transport early in infection remains uncertain. (Kondratova et al., 2005; Lukashok et al., 2000; Rasalingam et al., 2005; Tan et al., 2007; Ye et al., 2000).

The current study was initiated to define the mechanism by which incoming adenovirus recruits and uses dynein for its transport. Using a range of *in vivo* and *in vitro* assays, we find direct binding of adenovirus to dynein through its IC and LIC subunits. In contrast to physiological forms of cargo, we find no apparent role for dynactin in dynein recruitment to adenovirus, though we do detect a clear role in regulating virus transport. We identify hexon as the viral receptor for dynein, and find that hexon inhibition interferes with virus, but not physiological cargo transport. These results provide the first detailed mechanism for a virus-motor protein interaction, and identify a new avenue for potential therapeutic anti-viral intervention.

RESULTS

Association of dynein and its regulatory polypeptides with adenovirus *in situ*

To determine the extent to which dynein and its regulatory factors interact with adenovirus *in situ*, we compared their subcellular localization in fixed infected HeLa cells. A dynein HC-specific antibody that stains the Golgi apparatus (Roghi and Allan, 1999) clearly recognized

most (78%) adenovirus particles at 60 min p.i. (Fig 1A, D), well after escape of the virus from endosomes (Suomalainen et al., 1999). HC immunoreactivity was observed for capsids located within the cytoplasm and remained prominent on those that had already reached the nuclear envelope (supplemental Fig S1). A similarly high proportion of positive particles was found using antibodies to the dynactin subunits p150^{Glued} and Arp1, and to NudE/NudEL (Fig 1B–D). Somewhat lower colocalization of virus was observed for the dynein ICs, LC8, LICs, and NudC (Fig 1A, C, D), and little colocalization for LIS1, ZW10 (Fig 1C, D), or the early endosome marker EEA-1 (Fig 1 D, E). We also compared dynein HC staining of adenovirus at 15 min p.i. with clathrin distribution. Dynein HC was present only on viruses negative for clathrin (Fig 1F), indicating that dynein recruitment occurs only after exit of the virus from endosomes and, together with the EEA-1 results, confirming the specificity of dynein colocalization with adenovirus

Physical association of the adenovirus subunit hexon with dynein

We detected low levels of cytoplasmic dynein, but not dynactin, in immunoprecipitates of virus from infected A549 cell lysates at 40 min p.i. (Fig 2A). We also tested for dynein binding to the limited number of capsid subunits that might serve to recruit the motor protein. Of the three major proteins or protein complexes exposed on the virus surface, fiber is lost during transit through early endosomes, as has been reported for penton base, (Greber et al., 1993;Greber et al., 1996;Nakano et al., 2000;Matthews and Russell, 1998), though we do detect colocalization with post-endosomal and some nuclear envelope associated virus particles (Fig S2). Hexon remains a part of the capsid during transport to the nucleus and docking of virus particles with nuclear pore complexes. The minor capsid components proteins IIIa, VI, and VIII are lost or degraded prior to endosomal exit, and protein IX is substantially diminished during transit of the virus through the cytoplasm. Proteins V, VII and X are thought to remain within the virus core until nuclear entry or beyond. We, therefore, evaluated the behavior of five adenovirus capsid subunits : hexon, penton base, protein V, protein VII and protein X. We coexpressed 100K, a chaperone protein with hexon to ensure proper folding.

Proteins V and X and penton base were observed to be cytoplasmic when expressed in COS-7 cells (Fig S2) (Hong et al., 1999;Lee et al., 2003;Lee et al., 2004;Matthews and Russell, 1998), but coimmunoprecipitated neither dynein nor dynactin. Protein VII was exclusively nuclear (*op. cit.*) and was also negative in these assays.

Hexon was clearly cytoplasmic, but its transfection efficiency was too low to allow for reliable biochemical analysis. As an alternative approach we isolated hexon from late-stage Ad5-infected 293A cell lysates using a specific monoclonal antibody. The resulting preparations contained a single prominent band corresponding to the hexon monomer, as judged by Coomassie Blue staining and immunoblotting (Fig S3). In neutral buffers we found weak and variable interaction with dynein, which we noticed, however, to be enhanced at lower pH . To explore this effect further we exposed immunoisolated hexon to a series of pH conditions for 30 min, washed and resuspended the hexon in neutral buffer, and incubated hexon either with rat brain cytosol or purified rat brain cytoplasmic dynein for 1.5 hr. Cytoplasmic dynein could be readily detected in the pull-downs of hexon, which had been exposed to pH 4.4 (Fig 2C). Detection of both IC and LIC subunits in the pull-downs implied the presence of the complete dynein complex. Dynactin, NudE, and NudEL were absent from the pellets.

We also observed a clear interaction between hexon and purified cytoplasmic dynein (Fig 2D), which has been characterized extensively in our laboratory (Fig S6) (Paschal and Vallee, 1987). Hexon exposed to pH 4.4 pulled down 23% of total dynein. Hexon exposed to pH 5.4 pulled down somewhat less dynein, with little interaction observed for hexon exposed to higher pH values. An anti-dynein IC monoclonal antibody also coimmunoprecipitated MonoQ-purified hexon (Fig S6) (Waris and Halonen, 1987) which had been exposed to pH 4.4 (Fig

2E). These results confirm a direct hexon-dynein interaction and also indicate that the anti-dynein antibody, which we also use to block dynein function in cells (see below), does not abrogate the hexon-dynein interaction.

We tested further for an interaction between purified dynein and CsCl-purified adenovirus (Fig 2F). Consistent with our hexon results, short-term virus exposure to pH 4.4 strongly stimulated its interaction with dynein, with none detected using untreated virus (not shown).

To identify dynein components involved in adenovirus binding we overexpressed individual dynein subunits in COS-7 cells and tested to determine which were pulled down with low pH-treated hexon (Fig 3A–C). We observed strong interaction of full-length IC2C and LIC1 with hexon. LIC2 was present in the hexon pellets, but at background levels. No interaction with hexon was observed for the dynein light chains LC8, TxTex1, or RP3.

Comparison with physiological cargo-binding mechanisms

We also tested whether inhibition of physiological dynein regulatory and recruitment factors affected adenovirus behavior. As controls we found that a dynein HC RNAi (Tsai et al., 2007) expression of a dynein tail construct (Varma et al., 2006) or of the dynactin subunit dynamitin each potently inhibited virus redistribution to the nucleus (Fig S4, S5) , with a concentration toward the cell periphery in the latter case (Fig 4A), as observed for some minus-end vesicular organelles (Burkhardt et al., 1997). The Golgi apparatus was also disrupted in dynamitin-expressing cells (Burkhardt et al., 1997). Dynein HC was displaced from the Golgi elements under these conditions, as reported (Roghi and Allan, 1999; Varma et al., 2006), but persisted on a high percentage of virus particles (Fig 4A, D), consistent with a dynactin-independent mechanism of dynein recruitment to adenovirus. Expression of the CC1 fragment of the dynactin subunit p150^{Glued} (Quintyne et al., 1999) and an N-terminal p150^{Glued} deletion (ΔN- p150^{Glued}) lacking the microtubule binding domain (Kim et al., 2007) each potently inhibited virus redistribution to the nucleus (Fig S5, S6). ZW10 siRNA had no detectable effect on adenovirus redistribution to the nucleus (Fig 4C) or dynein HC colocalization with the virus, but showed the expected loss of HC from the Golgi apparatus (Varma et al., 2006) (Fig 4C, D). We also expressed a dominant negative C-terminal NudE cDNA and injected a function-blocking anti-NudE/NudEL antibody (Stehman et al., 2007) prior to virus infection with no effect virus redistribution to the nucleus (Fig 5A–C), nor, in the former case, on colocalization of dynein HC with virus particles (Fig 5D). Similarly, a dominant negative LIS1 construct and microinjection of a function-blocking anti-LIS1 antibody (Dujardin et al., 2003; Faulkner et al., 2000) had no appreciable effect in these assays (Fig 5A–D). Together these data indicate that neither ZW10, LIS1, NudE, nor NudEL are essential for either adenovirus transport to the nucleus or recruitment of dynein to the virus particles, despite the strong colocalization of NudE/NudEL in particular with incoming virus particles (Fig 1).

Physiological effects of hexon expression

To test the role of hexon in dynein recruitment and virus behavior *in vivo*, we expressed hexon in HeLa cells, and infected with adenovirus two days later. Hexon expression dramatically interfered with adenovirus redistribution to the nucleus, with adenovirus particles remaining dispersed throughout the cytoplasm in 65% of hexon-expressing cells (Fig 6A, B). Nonetheless, the Golgi apparatus was disrupted in only 26.5% of these cells, a level comparable to controls. Dynein HC colocalization with virus particles was also dramatically reduced (Fig 6C), but persisted at the Golgi apparatus (Fig 6D). In contrast, no effect on either virus distribution or the association of dynein with virus was observed in cells expressing adenovirus proteins V, VII , X, penton base, or 100K (Fig 6E, C). We note that hexon expression caused a limited degree of microtubule disorganization, especially toward the cell periphery (Fig 6F)). This

effect was unlikely to account for dispersal of adenovirus particles, as the Golgi apparatus remained compact and the microtubules were still largely focused around the centrosome.

A role for hexon in virus transport

To test how hexon perturbation might affect transport of incoming virions, we monitored Alexa 546-labeled Ad5 particles in infected cells by real-time fluorescence microscopy using COS-7 cells (Suomalainen et al., 1999), which have a more consistently radial microtubule cytoskeleton than HeLa cells. We were able to monitor virus movements continuously at video frame rate for up to a minute, to provide insight into individual virus "runs," as lower frame rates artificially merge runs into more continuous-appearing motility. Infected cells were recorded between 20 and 90 min p.i., and all actively moving viruses within a field were scored for direction of movement, run length, and velocity.

Hexon expression inhibited virus movement, but the partial distortion of the radial microtubule array in transfected cells reduced our ability to assign the direction of virus movement (data not shown). As an alternative approach we microinjected cells with monoclonal anti-hexon antibody and then infected the cells with Alexa-Ad5. Microtubule organization was unaffected (Fig 7A). In uninjected and control IgG-injected cells (Suppl. Movies 1,2), extensive virus movements were observed, with clearly detectable linear runs. Mean virus run lengths were approximately 600 nm for both inward and outward (microtubule minus end and plus end) directions (Fig 7C). Injection of anti-hexon antibody inhibited virus accumulation near the centrosome and reduced mean run lengths to approximately 350 nm in both directions (Fig 7B, C, D, Suppl. Movie 3). Velocity of transport was unaffected (Fig 7C). In contrast, lysosomal motility was largely unaffected (Fig S7B), though run length was slightly enhanced, as we also observe in controls (Fig 7C), possibly a reflection of cytoplasmic dilution by the injection solution. Injection of a monoclonal anti-dynein IC antibody prevented virus accumulation at the centrosome, as expected (Suppl. Movie 4) (Leopold et al., 2000). Mean run lengths were reduced to 270 nm, a decrease of more than 50%, again in both directions (see Discussion) (Fig 7C). A moderate increase in minus end velocity was observed.

We also observed a marked reduction in dynein HC colocalization with virus in the anti-hexon injected cells (Fig 7E, F), further supporting a role for hexon in dynein recruitment. In contrast, no significant reduction in dynein HC colocalization was observed in anti-dynein IC injected cells (Fig 7E, F). This result is consistent with the ability of the same antibody (74.1) to coimmunoprecipitate hexon with dynein (Fig 2E), and indicates that inhibition of virus motility in this case results not from loss of the motor protein but by interference with its regulation, as discussed below.

DISCUSSION

Although a number of viruses have been found to use cytoplasmic dynein to travel to the nucleus, how the motor protein is recruited for this purpose is poorly understood. We find that dynein binds directly to adenovirus through interactions between the dynein IC and LIC1 subunits and the capsid protein hexon. Dynactin plays a regulatory, but not a recruitment role in this system. Despite colocalization with virus particles *in situ* NudE and NudEL play no apparent role in virus transport, nor do LIS1 and ZW10. These results identify a mechanism for dynein recruitment to adenovirus that differs in significant ways from the better-established schemes for dynein recruitment to physiological forms of cargo, and identify at least one means to interfere selectively with pathogenic *vs* physiological aspects of cytoplasmic dynein function.

Role of hexon in direct dynein recruitment to virus

Hexon was the only one of five candidate capsid proteins that proved to interact with cytoplasmic dynein biochemically. Hexon interacted specifically with two dynein subunits, IC and LIC1, which reside within the cytoplasmic dynein tail and participate in linking dynein to physiological forms of cargo (Vaughan and Vallee, 1995; Karki and Holzbaur, 1995). The ICs, in particular, interact with both the dynactin complex (Vaughan and Vallee, 1995) and NudE (Stehman et al., 2007) Results from antibody injection experiments and from preliminary efforts to map the hexon binding site within the IC suggest that hexon binding is through a unique region of the IC (unpublished results). The interaction of hexon with more than one dynein subunit is unusual and suggests a potentially cooperative interaction with multiple sites on the surface of the motor protein complex.

An unusual feature of the virus-dynein interaction is its activation by exposure of the virus proteins to low pH. This behavior is very much in keeping with effects of the acidic endosomal environment on virus composition and on the conformation of constituent subunits. We observe a comparable effect of low pH exposure on the interaction of both virus and isolated hexon with dynein. The final pH reached in the adenovirus-containing endosome has been determined at ≤ 5.5 (Martin-Fernandez et al., 2004), suggesting that our biochemical results reflect a real pathophysiological mechanism to prime virus for dynein recruitment. Such a mechanism could serve not only to activate transport toward the nucleus early in the infectious cycle, but also to prevent transport of virus components later on.

To test further for a role specifically in incoming capsid transport rather than in some other stage in the infectious cycle, we examined the effects of hexon expression and anti-hexon antibody injection on virus behavior. Each treatment prevented virus accumulation at the centrosome and nucleus. Furthermore, in each case, the percentage of adenovirus particles staining positively for dynein was also greatly reduced. These results provide further evidence for a role for hexon in dynein recruitment *per se*. Dynactin and NudE/NudEL were also displaced from virus by hexon expression. Whilst these observations could serve as evidence that hexon may interact independently with these dynein-interacting proteins, another interpretation is that NudE/NudEL and dynactin are linked to the virus indirectly through dynein (Fig 7G). This possibility is, indeed, supported by our biochemical data, which show no evidence for a direct interaction of dynactin and NudE/NudEL with virus.

To test more directly for a role for hexon in dynein-mediated motility, we analyzed the behavior of virus in living COS-7 cells. In these cells, adenovirus tends to accumulate at the centrosome before redistributing to the nuclear envelope (Strunze et al., 2005). We monitored virus movement continuously, and analyzed all directionally moving particles (see Supplemental Materials and Methods) within a given cell for the duration of each movie. Injection of anti-hexon antibody significantly reduced mean virus run length, an effect consistent with either reduced motor protein number at the virus surface or altered motor protein regulation, though the marked reduction in dynein HC colocalization with adenovirus supports the former possibility. Minus end-directed virus velocity was unaffected, consistent with evidence that motor number does not affect the rate of cargo movement.

Regulation of dynein-mediated virus transport

In contrast, the observed effect of anti-dynein IC antibody injection on virus motility may, indeed, reflect changes in dynein regulation. This treatment reduced mean virus run length without displacing dynein HC from adenovirus. This result implies that the antibody and hexon interact with different sites within the dynein IC, a result supported by anti-IC coimmunoprecipitation of hexon with dynein (Fig 2E). Anti-IC antibodies do tend, however, to interact with the N-terminus of the IC and affect the interaction of dynein with dynactin

(Vaughan and Vallee, 1995). Therefore, as dynein HC remained on the virus in anti-IC-injected cells, inhibition of dynein-mediated adenovirus motility is more reasonably explained in this case by interference with the dynein-dynactin interaction than with dynein recruitment to virus particles.

Both inward and outward directions of adenovirus movement were affected to a similar extent in anti-hexon injected cells. This observation could indicate a role for hexon in recruitment of both minus end-directed and plus end-directed microtubule motor proteins to the adenovirus capsid. However, injection of anti-dynein IC antibody also affected both directions of movement. The observed motility effects could, therefore, indicate a role for dynein in bidirectional transport, a possibility raised by recently reported analysis of isolated dynein molecules *in vitro* (Ross et al., 2006). Alternatively, our results are in line with reports of functional coupling between minus-end and plus-end transport (Gross et al., 2002; Kim et al., 2007), in which alteration of transport in one direction also results in changes in transport in the opposite direction. The underlying mechanism for these effects remains uncertain.

Dynactin is the best characterized of the dynein regulatory factors and has previously been implicated in adenovirus transport to the nucleus (Suomalainen et al., 1999). We detect dynactin on a very high proportion of incoming adenovirus capsids by immunocytochemistry. However, the absence of dynactin in hexon and adenovirus immunoprecipitates and the failure of dynamitin overexpression to decrease dynein colocalization with adenovirus, in contrast to mitotic kinetochores and the Golgi apparatus (Burkhardt et al., 1997; Echeverri et al., 1996; Roghi and Allan, 1999), argue further that the well-established role for dynactin in dynein recruitment does not apply to adenovirus. Thus, our results together lead to the conclusion that dynactin plays only a regulatory role in adenovirus transport.

NudE and NudEL have also recently been implicated in dynein recruitment to kinetochores and centrosomes (Guo et al., 2006; Liang et al., 2007; Stehman et al., 2007; Vergnolle and Taylor, 2007) and we observed NudE/NudEL immunoreactivity on a high proportion of incoming adenovirus capsids. Nonetheless, inhibition of these proteins using reagents previously found to inhibit mitosis (Stehman et al., 2007) had no effect on adenovirus accumulation at the nucleus or on dynein recruitment to the virus. NudE/NudEL, therefore, seem not to be essential for transport of the incoming virions.

LIS1 is a dynein-, NudE- and NudEL- interacting protein that has received considerable attention for its role in the brain developmental disease lissencephaly, which functions with dynein in cell division and migration (Dujardin et al., 2003; Faulkner et al., 2000; Tsai et al., 2005). However, we saw little colocalization of LIS1 with incoming adenovirus, and inhibitory reagents had no effect on virus accumulation at the nucleus or recruitment of dynein to the virus, suggesting that LIS1 does not participate in dynein-mediated adenovirus transport.

ZW10 binds dynactin, which in turn anchors dynein at kinetochores as well as at the Golgi apparatus (Starr et al., 1998; Varma et al., 2006; Whyte et al., 2008). ZW10 also participates in many other dynein functions. The lack of effect of. ZW10 knockdown on dynein HC colocalization with Ad5 or virus transport to the nucleus indicates that dynein recruitment by adenovirus is independent of ZW10, and, in turn, supports a dynactin-independent model for dynein recruitment to the virus.

Our results together argue against a role for known dynein recruitment factors – dynactin, NudE/NudEL, and ZW10 - in linking dynein to adenovirus. Nonetheless, dynactin inhibition does affect virus redistribution, strongly supporting a role as a regulator of motor activity and processivity. Adenovirus transport thus provides the first example of dynein-mediated transport involving the dynactin complex solely in motor regulation. In the case of NudE and

NudEL, whether these proteins bind passively to virus-associated dynein or have more subtle effects on the efficiency of transport remains to be investigated.

Mechanism of dynein recruitment to adenovirus

Our results lead to a model for direct dynein recruitment to adenovirus through hexon, with dynactin linked to the capsid *via* dynein, the reverse of the normal cargo-binding situation (Fig 7G). The unique aspects of the adenovirus-dynein interaction may also enable design of novel therapeutic strategies with minimal physiological consequences. We find in particular that hexon expression and anti-hexon antibody injection have no apparent effect on the organization of the Golgi apparatus, a commonly used indicator of physiological dynein function (Burkhardt et al., 1997). Furthermore, whilst dynein was displaced from adenovirus particles by hexon expression or antibody inhibition, it remained present on the Golgi apparatus. Thus, reagents could potentially be designed which interfere with adenovirus transport without physiological effect.

Our results identify a novel dynein cargo binding mechanism. Whether it applies more generally to invading pathogens remains an important question for future investigation.

EXPERIMENTAL PROCEDURES

Cells, Viruses, and Molecular Methods

HeLa, A549, COS-7 and 293A cells were grown in DME supplemented with 10% FBS. Antibodies and plasmids are described in Supplemental Methods. Replication-deficient Ad5 expressing GFP (plaque-purified; obtained from H. Young, Columbia University, NY) was propagated in 293A cells and purified by CsCl banding as described (Mautner, 1999). The virus-depleted lysate was recovered and used for hexon immunoprecipitation (see below). Viral titer was obtained using fluorescent focus and plaque assays. Ad5 was labeled with Cy3 or Alexa Fluor 546 (Invitrogen) for live cell imaging experiments as described (Leopold et al., 1998).. Infectivity and nuclear accumulation of the virus were unaffected by fluorophore conjugation (data not shown). Lysotracker-red (Invitrogen) was used to label lysosomes. Transient transfections were performed using either Fugene (Roche), Lipofectamine 2000 (Invitrogen Corp.) or Effectene (QIAGEN). Adenovirus infections (m. o. i. 100 for microscopy, 1000 for biochemical analysis) were all performed in a low volume of DME containing 2% FBS at 4°C for 40 min to allow virus attachment. The cells were washed twice in cold PBS and incubated in fresh DME/2% FBS for 60 min at 37°C, unless stated otherwise, to allow internalization and intracellular transport.

Biochemical analysis

Rat brain lysate and purified rat cytoplasmic dynein were prepared in phosphate-glutamate buffer pH 7.0 as previously described (Fig S5)(Paschal et al., 1987). Unless stated otherwise, mammalian cultured cell lysates were prepared in RIPA buffer (100 mM NaCl, 1 mM EGTA, 50 mM Tris base; pH 8) containing 1% NP40, and the membrane fraction removed by centrifugation. Adenoviral polypeptides were expressed in COS-7 cells. Additional detergent extraction in RIPA/1% Triton X-100 was required for analysis of protein X-GFP expression and nuclear extracts were prepared for analysis of protein VII expression (Dignam et al., 1983). The hexon polypeptide required coexpression of its 100K chaperone polypeptide. Formation of the native hexon trimer and penton base pentamer was confirmed by immunoblotting of unboiled samples treated with benzonase at 37°C for 10 min (Fig S2). Dynein and dynactin pull-downs were performed by 2 h incubation with protein G-sepharose blocked with 0.2 mg ml^{-1} BSA in 0.1% Triton X-100/PBS. Interacting proteins were identified by immunoblotting. In experiments in which late-stage infected cell lysate was used, hexon was immunoprecipitated using a monoclonal antibody. The resulting preparations contained a

single prominent band corresponding to the hexon monomer, in addition to the antibody heavy and light chains, as judged by Coomassie Blue staining and immunoblotting (Fig S3). The hexon beads were washed and incubated for 30 min in Tris-maleate buffer (50 mM Trizma-maleate, 10 mM NaCl, 1 mM EDTA, and 0.1% Tween20, pH 4.4–7.4 as indicted), washed in the same buffer at pH 7.4, and then incubated with purified cytoplasmic dynein, bovine brain lysate or cell lysate for 1.5 h. Following extensive washing, the beads were analyzed for the presence of dynein by immunoblotting.

Immunofluorescence microscopy

Cells were grown on glass coverslips and fixed in methanol at −20°C for 5 min. In some cases, cells were pre-extracted in 0.5% Triton X-100 in PHEM buffer (120 mM Pipes, 50 mM Hepes, 20 mM EGTA, and 4 mM magnesium acetate) for 1 min at room temperature. Coverslips were blocked for 30 min in 0.5% BSA/PBS, incubated in primary antibody at 37°C for 1 h, washed and incubated for 1 h at 37°C in Cy2-, Cy3- or Cy5-conjugated secondary antibody, then stained with DAPI for 10 min to visualize DNA. Coverslips were mounted using ProLong Gold Anti-fade mounting media (Invitrogen) and imaged using either a Leica DM IRBE inverted microscope equipped with a CCD camera (ORCA 100, Hamamatsu) and a 63× oil immersion objective, or by confocal imaging (510 META, Carl Zeiss MicroImaging Inc.) using a 100× oil immersion objective. For quantification of colocalization of cellular polypeptides with intracellular adenovirus, virus particles in 10 cells from each of three independent experiments were analyzed for each antigen. Only instances in which there was a discrete dynein signal directly coinciding with the virus signal were counted as positive colocalization. The percentage of incoming virus particles that were positive for each antigen was calculated.

Microinjection and live cell imaging

For all live cell imaging experiments, cells were grown in glass-bottomed dishes (MatTek Corp.). For antibody injection, a purified IgG fraction of monoclonal anti-hexon, monoclonal anti-dynein IC (Leopold et al., 2000) or polyclonal anti-NudE/NudEL (Stehman et al., 2007) or anti-LIS1 (Faulkner et al., 2000) was concentrated in microinjection buffer (10 mM HEPES pH 7.4 containing 140 mM KCl). Injections were performed with the cells in a 37°C chamber with a 5% CO_2 atmosphere and using a micromanipulator (model 5171; Eppendorf). Cells were allowed to recover at 37°C for 10 min in new medium, infected after at least 15 min with fluorescently-labeled Ad5, and then processed for live cell imaging or immunocytochemistry to test for effects on virus and organelle distribution and for the presence of the injected antibody. Movies were acquired 20–90 min p.i. using a 100× oil immersion objective (actual pixel size ~160 nm/pixel) and a CCD camera (model C9100-12; Hamamatsu) attached to an inverted microscope (IX80; Olympus). We exposed the cells continuously for 1 min with a video rate of 16 frames/sec and using the Metamorph stream acquisition function. At 90 min p.i., cells were fixed in ice-cold methanol and processed for immunocytochemistry.

Statistical analysis

For the motility analysis, two-sample comparisons were performed via both Student t-test and Wilcoxon ranksum test. In all other cases, the Student t-test alone was used. Statistical significance was inferred for *P* values less than 0.05 for both tests. All statistical tests were performed using Matlab (Mathworks, Natick, Mass) and Origin (Microcal Software, Northampton, MA).

Supplementary Material

Refer to Web version on PubMed Central for supplementary material.

Acknowledgments

We are grateful to R. McKenney for preparation of purified dynein from rat brain, S. Stehman for purification of NudE/NudEL and LIS1 antibodies and for some antibody injections, and S. Tan for production of the anti-LIC1 antibody. We thank D.A. Matthews, P. Boulanger, L. Gerace, V. Allan, B. Schaar, D. Meyer, K. Vaughan, K. Pfister, M.L. Goldberg, H. Young, G. Duijou, and T. Schroer for antibodies, plasmids, adenovirus, cell lines or helpful discussion. This work was supported by National Institutes of Health grants GM47434 to RV, GM 64624 to SPG and an American Heart Association Heritage Affiliate Postdoctoral Fellowship (KHB).

REFERENCES

Alonso C, Miskin J, Hernaez B, Fernandez-Zapatero P, Soto L, Canto C, Rodriguez-Crespo I, Dixon L, Escribano JM. African swine fever virus protein p54 interacts with the microtubular motor complex through direct binding to light-chain dynein. J Virol 2001;75:9819–9827. [PubMed: 11559815]

Burkhardt JK, Echeverri CJ, Nilsson T, Vallee RB. Overexpression of the dynamitin (p50) subunit of the dynactin complex disrupts dynein-dependent maintenance of membrane organelle distribution. J Cell Biol 1997;139:469–484. [PubMed: 9334349]

Cotten M, Weber JM. The adenovirus protease is required for virus entry into host cells. Virology 1995;213:494–502. [PubMed: 7491774]

Dignam JD, Martin PL, Shastry BS, Roeder RG. Eukaryotic gene transcription with purified components. Methods Enzymol 1983;101:582–598. [PubMed: 6888276]

Dohner K, Nagel CH, Sodeik B. Viral stop-and-go along microtubules: taking a ride with dynein and kinesins. Trends Microbiol 2005;13:320–327. [PubMed: 15950476]

Dujardin DL, Barnhart LE, Stehman SA, Gomes ER, Gundersen GG, Vallee RB. A role for cytoplasmic dynein and LIS1 in directed cell movement. J Cell Biol 2003;163:1205–1211. [PubMed: 14691133]

Echeverri CJ, Paschal BM, Vaughan KT, Vallee RB. Molecular characterization of the 50kD subunit of dynactin reveals function for the complex in chromosome alignment and spindle organization during mitosis. J Cell Biol 1996;132:617–633. [PubMed: 8647893]

Faulkner NE, Dujardin DL, Tai CY, Vaughan KT, O'Connell CB, Wang Y, Vallee RB. A role for the lissencephaly gene LIS1 in mitosis and cytoplasmic dynein function. Nat Cell Biol 2000;2:784–791. [PubMed: 11056532]

Greber UF, Way M. A superhighway to virus infection. Cell 2006;124:741–754. [PubMed: 16497585]

Greber UF, Webster P, Weber J, Helenius A. The role of the adenovirus protease on virus entry into cells. Embo J 1996;15:1766–1777. [PubMed: 8617221]

Greber UF, Willetts M, Webster P, Helenius A. Stepwise dismantling of adenovirus 2 during entry into cells. Cell 1993;75:477–486. [PubMed: 8221887]

Gross SP, Welte MA, Block SM, Wieschaus EF. Coordination of opposite-polarity microtubule motors. J Cell Biol 2002;156:715–724. [PubMed: 11854311]

Guo J, Yang Z, Song W, Chen Q, Wang F, Zhang Q, Zhu X. Nudel contributes to microtubule anchoring at the mother centriole and is involved in both dynein-dependent and -independent centrosomal protein assembly. Mol Biol Cell 2006;17:680–689. [PubMed: 16291865]

Hong SS, Gay B, Karayan L, Dabauvalle MC, Boulanger P. Cellular uptake and nuclear delivery of recombinant adenovirus penton base. Virology 1999;262:163–177. [PubMed: 10489350]

Jacob Y, Badrane H, Ceccaldi PE, Tordo N. Cytoplasmic dynein LC8 interacts with lyssavirus phosphoprotein. J Virol 2000;74:10217–10222. [PubMed: 11024152]

Karki S, Holzbaur ELF. Affinity chromatography demonstrates a direct binding between cytoplasmic dynein and the dynactin complex. J Biol Chem 1995;270:28806–28811. [PubMed: 7499404]

Kelkar S, De BP, Gao G, Wilson JM, Crystal RG, Leopold PL. A common mechanism for cytoplasmic dynein-dependent microtubule binding shared among adeno-associated virus and adenovirus serotypes. J Virol 2006;80:7781–7785. [PubMed: 16840360]

Kelkar SA, Pfister KK, Crystal RG, Leopold PL. Cytoplasmic dynein mediates adenovirus binding to microtubules. J Virol 2004;78:10122–10132. [PubMed: 15331745]

Kim H, Ling SC, Rogers GC, Kural C, Selvin PR, Rogers SL, Gelfand VI. Microtubule binding by dynactin is required for microtubule organization but not cargo transport. J Cell Biol 2007;176:641–651. [PubMed: 17325206]

King SJ, Schroer TA. Dynactin increases the processivity of the cytoplasmic dynein motor. Nat Cell Biol 2000;2:20–24. [PubMed: 10620802]

Kondratova AA, Neznanov N, Kondratov RV, Gudkov AV. Poliovirus protein 3A binds and inactivates LIS1, causing block of membrane protein trafficking and deregulation of cell division. Cell Cycle 2005;4:1403–1410. [PubMed: 16138011]

Lee TW, Blair GE, Matthews DA. Adenovirus core protein VII contains distinct sequences that mediate targeting to the nucleus and nucleolus, and colocalization with human chromosomes. J Gen Virol 2003;84:3423–3428. [PubMed: 14645923]

Lee TW, Lawrence FJ, Dauksaite V, Akusjarvi G, Blair GE, Matthews DA. Precursor of human adenovirus core polypeptide Mu targets the nucleolus and modulates the expression of E2 proteins. J Gen Virol 2004;85:185–196. [PubMed: 14718634]

Leopold PL, Ferris B, Grinberg I, Worgall S, Hackett NR, Crystal RG. Fluorescent virions: dynamic tracking of the pathway of adenoviral gene transfer vectors in living cells. Hum Gene Ther 1998;9:367–378. [PubMed: 9508054]

Leopold PL, Kreitzer G, Miyazawa N, Rempel S, Pfister KK, Rodriguez-Boulan E, Crystal RG. Dynein- and microtubule-mediated translocation of adenovirus serotype 5 occurs after endosomal lysis. Hum Gene Ther 2000;11:151–165. [PubMed: 10646647]

Liang Y, Yu W, Li Y, Yu L, Zhang Q, Wang F, Yang Z, Du J, Huang Q, Yao X, Zhu X. Nudel modulates kinetochore association and function of cytoplasmic dynein in M phase. Mol Biol Cell 2007;18:2656–2666. [PubMed: 17494871]

Lukashok SA, Tarassishin L, Li Y, Horwitz MS. An adenovirus inhibitor of tumor necrosis factor alpha-induced apoptosis complexes with dynein and a small GTPase. J Virol 2000;74:4705–4709. [PubMed: 10775608]

Martin-Fernandez M, Longshaw SV, Kirby I, Santis G, Tobin MJ, Clarke DT, Jones GR. Adenovirus type-5 entry and disassembly followed in living cells by FRET, fluorescence anisotropy, and FLIM. Biophys J 2004;87:1316–1327. [PubMed: 15298934]

Matthews DA, Russell WC. Adenovirus core protein V is delivered by the invading virus to the nucleus of the infected cell and later in infection is associated with nucleoli. J Gen Virol 1998;79(Pt 7):1671–1675. [PubMed: 9680130]

Mautner, V. Methods for growth and purification of enteric adenovirus type 40 Adenovirus. In: WSM, W., editor. Adenovirus Methods and Protocols. New Jersey: Humana Press; 1999. p. 283-294.

Nakano MY, Boucke K, Suomalainen M, Stidwill RP, Greber UF. The first step of adenovirus type 2 disassembly occurs at the cell surface, independently of endocytosis and escape to the cytosol. J Virol 2000;74:7085–7095. [PubMed: 10888649]

Paschal BM, Shpetner HS, Vallee RB. MAP 1C is a microtubule-activated ATPase which translocates microtubules *in vitro* and has dynein-like properties. J Cell Biol 1987;105:1273–1282. [PubMed: 2958482]

Paschal BM, Vallee RB. Retrograde transport by the microtubule associated protein MAP 1C. Nature 1987;330:181–183. [PubMed: 3670402]

Quintyne NJ, Gill SR, Eckley DM, Crego CL, Compton DA, Schroer TA. Dynactin is required for microtubule anchoring at centrosomes. J Cell Biol 1999;147:321–334. [PubMed: 10525538]

Rasalingam P, Rossiter JP, Mebatsion T, Jackson AC. Comparative pathogenesis of the SAD-L16 strain of rabies virus and a mutant modifying the dynein light chain binding site of the rabies virus phosphoprotein in young mice. Virus Res 2005;111:55–60. [PubMed: 15896402]

Roghi C, Allan VJ. Dynamic association of cytoplasmic dynein heavy chain 1a with the Golgi apparatus and intermediate compartment. J Cell Sci 1999;112(Pt 24):4673–4685. [PubMed: 10574715]

Ross JL, Wallace K, Shuman H, Goldman YE, Holzbaur EL. Processive bidirectional motion of dynein-dynactin complexes in vitro. Nat Cell Biol 2006;8:562–570. [PubMed: 16715075]

Sodeik B, Ebersold MW, Helenius A. Microtubule-mediated transport of incoming herpes simplex virus 1 capsi ds to the nucleus. J Cell Biol 1997;136:1007–1021. [PubMed: 9060466]

Starr DA, Williams BC, Hays TS, Goldberg ML. ZW10 helps recruit dynactin and dynein to the kinetochore. J Cell Biol 1998;142:763–774. [PubMed: 9700164]

Stehman SA, Chen Y, McKenney RJ, Vallee RB. NudE and NudEL are required for mitotic progression and are involved in dynein recruitment to kinetochores. J Cell Biol 2007;178:583–594. [PubMed: 17682047]

Strunze S, Trotman LC, Boucke K, Greber UF. Nuclear targeting of adenovirus type 2 requires CRM1-mediated nuclear export. Mol Biol Cell 2005;16:2999–3009. [PubMed: 15814838]

Suikkanen S, Aaltonen T, Nevalainen M, Valilehto O, Lindholm L, Vuento M, Vihinen-Ranta M. Exploitation of microtubule cytoskeleton and dynein during parvoviral traffic toward the nucleus. J Virol 2003;77:10270–10279. [PubMed: 12970411]

Suomalainen M, Nakano MY, Keller S, Boucke K, Stidwill RP, Greber UF. Microtubule-dependent plus- and minus end-directed motilities are competing processes for nuclear targeting of adenovirus. J Cell Biol 1999;144:657–672. [PubMed: 10037788]

Tan GS, Preuss MA, Williams JC, Schnell MJ. The dynein light chain 8 binding motif of rabies virus phosphoprotein promotes efficient viral transcription. Proc Natl Acad Sci U S A 2007;104:7229–7234. [PubMed: 17438267]

Trotman LC, Mosberger N, Fornerod M, Stidwill RP, Greber UF. Import of adenovirus DNA involves the nuclear pore complex receptor CAN/Nup214 and histone H1. Nat Cell Biol 2001;3:1092–1100. [PubMed: 11781571]

Tsai JW, Bremner KH, Vallee RB. Dual subcellular roles for LIS1 and dynein in radial neuronal migration in live brain tissue. Nat Neurosci 2007;10:970–979. [PubMed: 17618279]

Tsai JW, Chen Y, Kriegstein AR, Vallee RB. LIS1 RNA interference blocks neural stem cell division, morphogenesis, and motility at multiple stages. J Cell Biol 2005;170:935–945. [PubMed: 16144905]

Varma D, Dujardin DL, Stehman SA, Vallee RB. Role of the kinetochore/cell cycle checkpoint protein ZW10 in interphase cytoplasmic dynein function. J Cell Biol 2006;172:655–662. [PubMed: 16505164]

Vaughan KT, Vallee RB. Cytoplasmic dynein binds dynactin through a direct interaction between the intermediate chains and p150 ^{Glued}. J Cell Biol 1995;131:1507–1516. [PubMed: 8522607]

Vergnolle MA, Taylor SS. Cenp-F links kinetochores to Ndel1/Nde1/Lis1/dynein microtubule motor complexes. Curr Biol 2007;17:1173–1179. [PubMed: 17600710]

Whyte J, Bader JR, Tauhata SB, Raycroft M, Hornick J, Pfister KK, Lane WS, Chan GK, Hinchcliffe EH, Vaughan PS, Vaughan KT. Phosphorylation regulates targeting of cytoplasmic dynein to kinetochores during mitosis. J Cell Biol 2008;183:819–834. [PubMed: 19029334]

Wiethoff CM, Wodrich H, Gerace L, Nemerow GR. Adenovirus protein VI mediates membrane disruption following capsid disassembly. J Virol 2005;79:1992–2000. [PubMed: 15681401]

Ye GJ, Vaughan KT, Vallee RB, Roizman B. The herpes simplex virus 1 U(L)34 protein interacts with a cytoplasmic dynein intermediate chain and targets nuclear membrane [In Process Citation]. J Virol 2000;74:1355–1363. [PubMed: 10627546]

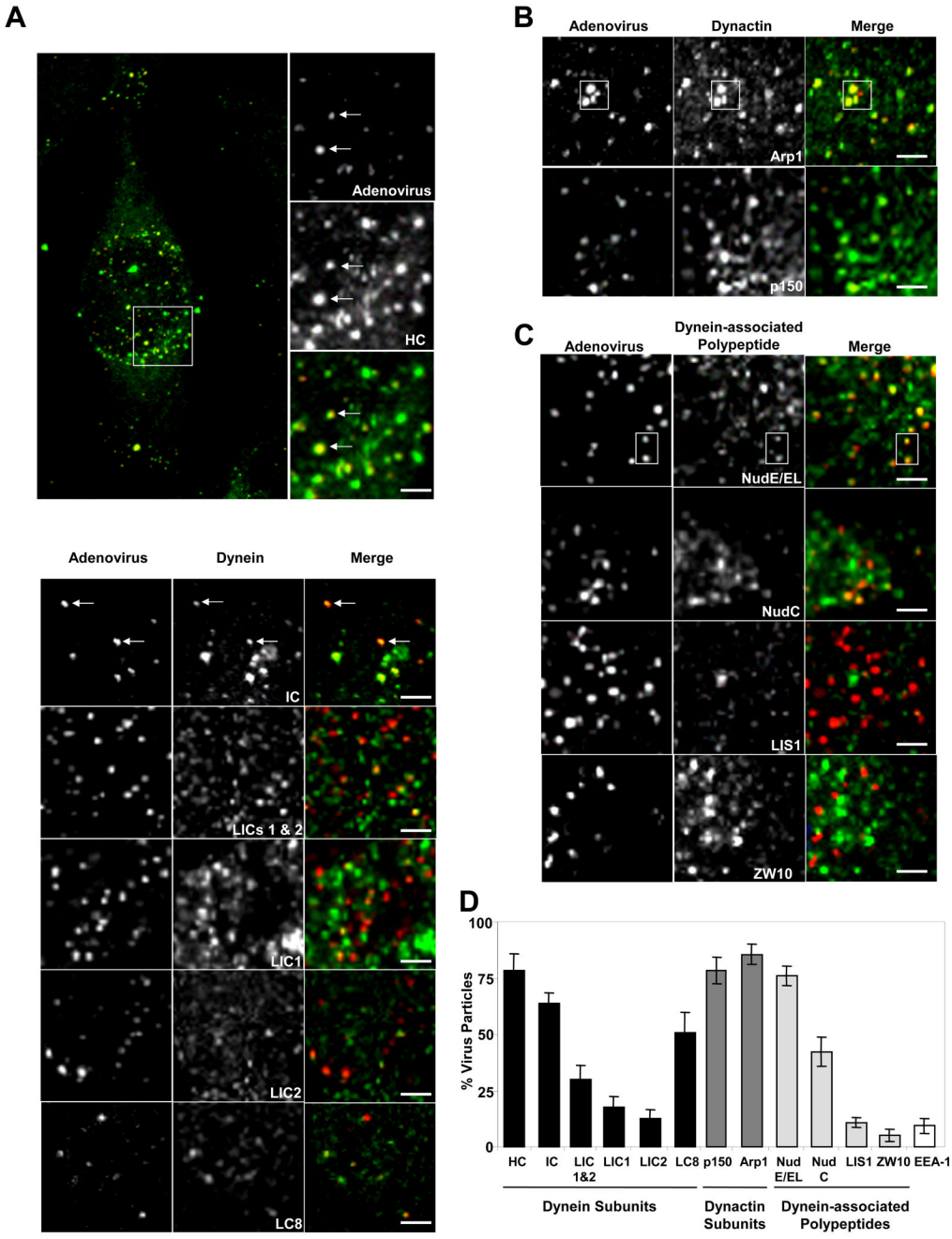

Figure 1. Colocalization of cytoplasmic dynein and associated factors with incoming adenovirus capsids *in situ*

HeLa cells were infected with Ad5 (red) for 60 min and processed for immunofluorescence microscopy using antibodies (green) to (**A**) dynein, (**B**) dynactin, or (**C**) dynein regulatory proteins. A whole cell is shown in **A**, as well as expanded regions from confocal images of Ad5 chemically labeled with Cy3 (See Fig S1 for additional whole cell images.). Arrows or boxed regions highlight examples of virus colocalization with dynein and other antigens. All images are merged stacks and the scale bars represent 1μm. (**D**) Percentage of Ad5 particles +/− SD staining positively for costained markers. Virus particles in 10 cells from each of three independent experiments were analyzed for each antigen. (**E**) Double labeling of adenovirus

at 60 min p.i. with the early endosomal marker EEA-1 (green), showing low colocalization. (**F**) Triple labeling of adenovirus at 15 min p.i with anti-dynein HC and anti-clathrin. Arrows show examples of HC-positive virus particles which are negative for clathrin, consistent with recruitment of dynein after exit of the virus from the early endosome. The panels show the same region of the same cell with dynein HC (green) on the left and clathrin (green) on the right.

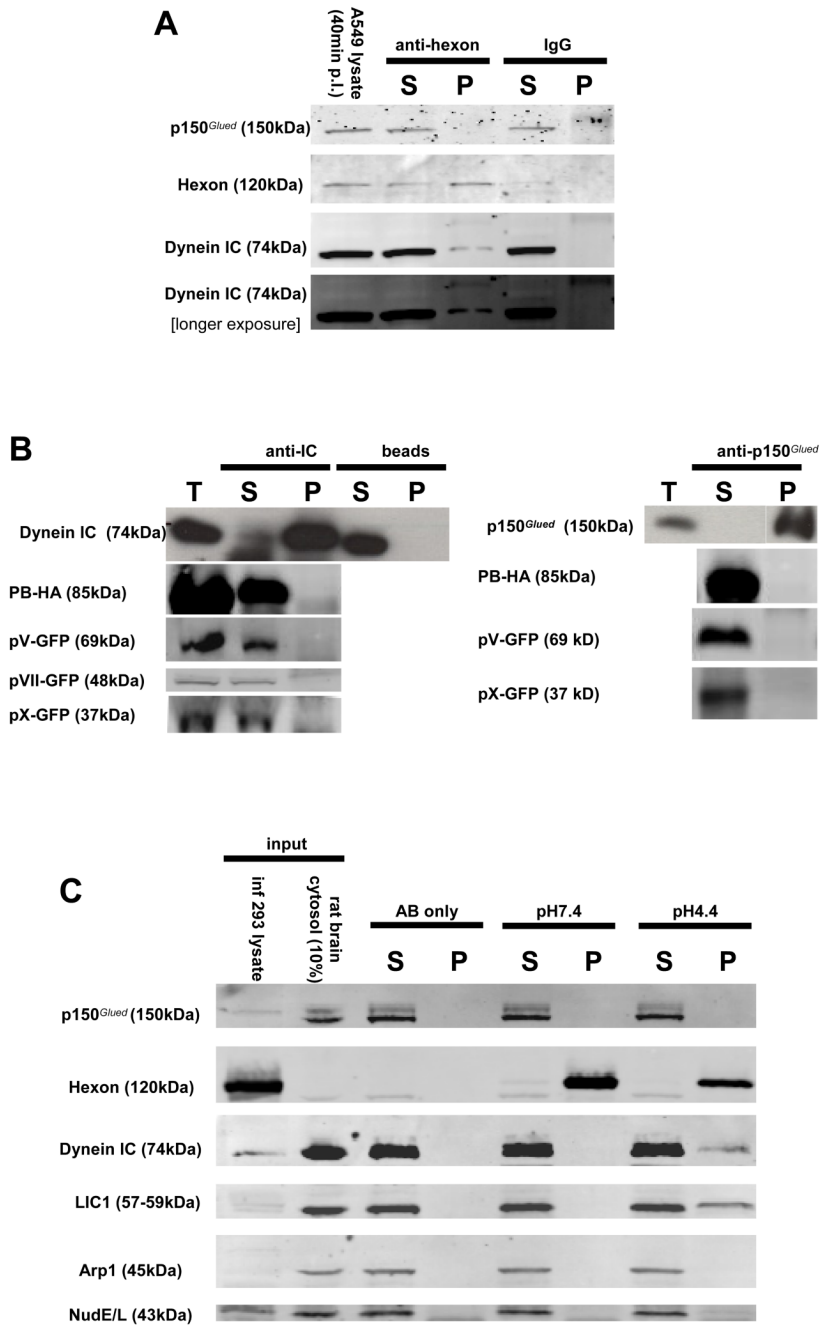

Figure 2. Adenovirus interacts with dynein, but not dynactin, via the hexon capsid subunit

(**A**) Ad5 was immunoprecipitated from infected A549 cell lysate 40min p.i. and the pellets were immunoblotted using anti-dynein IC or anti-dynactin p150^{Glued} antibodies. Dynein but not dynactin was present in the pellets. (**B**) Dynein (IC) and dynactin (p150^{Glued}) were immunoprecipitated from lysates of COS-7 cells expressing the recombinant viral capsid polypeptides protein V, penton base, and proteins VII and X, none of which were found in the pellets. (**C**) Analysis of dynein and dynactin binding to hexon. Hexon was immunoprecipitated from infected 293A cell lysates, exposed to pH 7.4 or pH 4.4 buffer for 30 min, and then returned to pH 7.4, mixed with rat brain cytosol, and immunoprecipitated. The dynein complex, detected by blotting for IC and LIC1 subunits, clearly bound to the pH 4.4-treated, but not the

control hexon. The dynactin complex, detected by blotting for p150^{Glued} and Arp1 subunits, was absent in both cases, as were NudE and NudEL. (**D**) Hexon was exposed to a range of pH values, washed at pH 7.4, incubated with purified rat brain cytoplasmic dynein, and immunoprecipitated. The purified cytoplasmic dynein showed a pH-dependent interaction with hexon, which increased markedly with hexon exposure to decreasing pH. (**E**) Purified rat brain cytoplasmic dynein was bound to anti-dynein IC antibody 74.1 and incubated with pH 4.4 pretreated hexon purified by anion exchange chromatography from adenovirus infected cell lysates. Hexon was clearly present in the dynein pellet. (**F**) Immunopurified (IPed) hexon or intact adenovirus was acidified at pH 4.4, restored to pH 7.4, incubated with purified rat brain cytoplasmic dynein, and immunoprecipitated. The dynein complex as revealed by staining with anti- HC, IC, LIC1, and LIC2 antibodies was clearly present in both the hexon and adenovirus pellets. T (total), S (supernatant), and P (pellet)

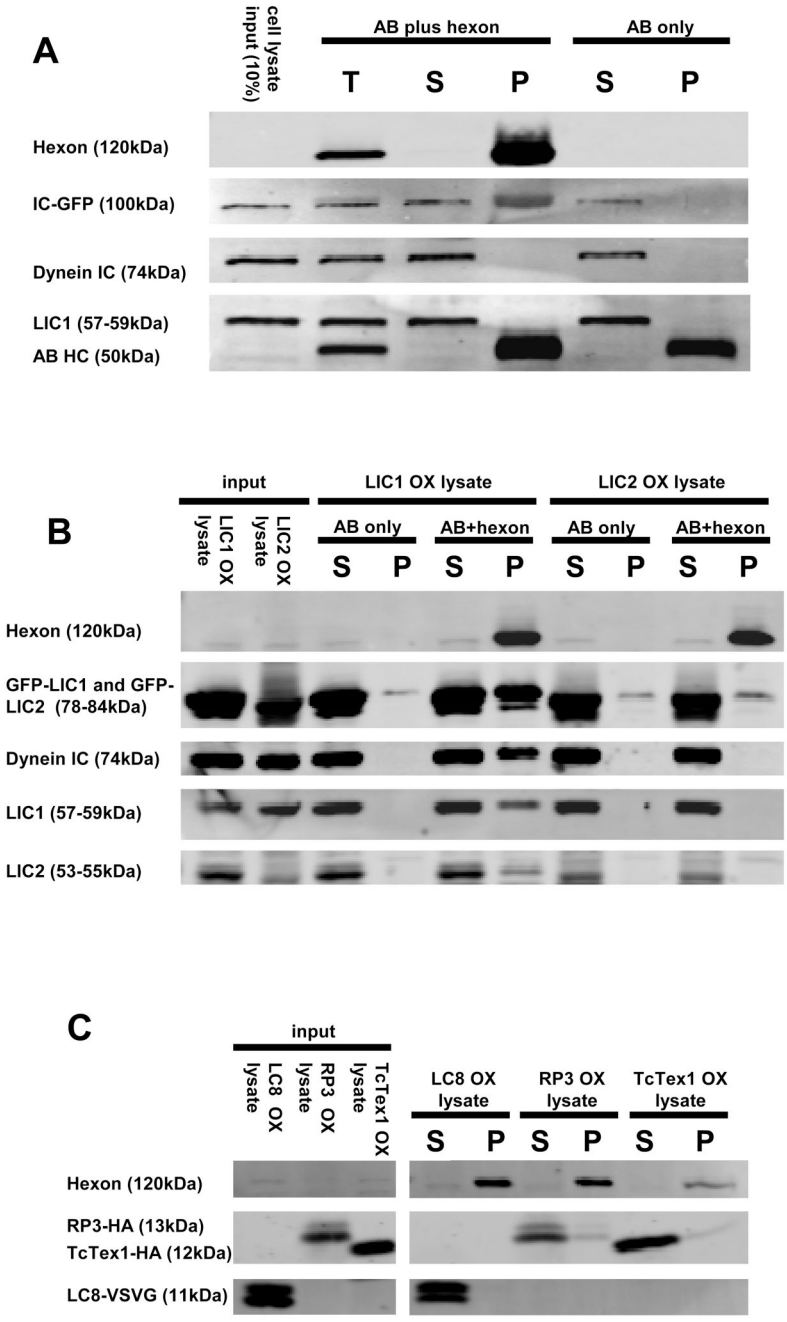

Figure 3. Hexon interacts with dynein IC and LIC1

Hexon was immunoisolated from late stage adenovirus infected 293A cell lysates, exposed to pH 4.4, and combined at pH 7.4 with lysates of COS-7 cells expressing individual dynein subunits. (**A**) Hexon pull-downs from IC2C-GFP-expressing cell lysates were blotted with antibodies to dynein IC and LIC1. The recombinant IC-GFP at 100kDa clearly associated with hexon. The lack of immunoreactivity at the positions of the endogenous IC and LIC1 indicates that endogenous dynein was present at too low levels to be detected. (**B**) Hexon pull-downs from LIC1-GFP- or LIC2-GFP-expressing cell lysates were blotted with anti-GFP, plus anti-IC, -LIC1, and LIC2 antibodies. The recombinant LIC1-GFP clearly associated with hexon. In this experiment endogenous dynein complex also bound to hexon as indicated by the

presence of all three dynein antigens in the hexon pull-down. Recombinant LIC2 showed little to no hexon binding relative the antibody-only control. (**C**) Hexon pull-downs from LC8-VSVG-, RP3-HA-, or TcTex1-HA-expressing cell lysates were blotted with antibodies to the respective epitope tags. None of the three recombinant LCs bound to hexon. OX (overexpression), T (total), S (supernatant), and P (pellet)

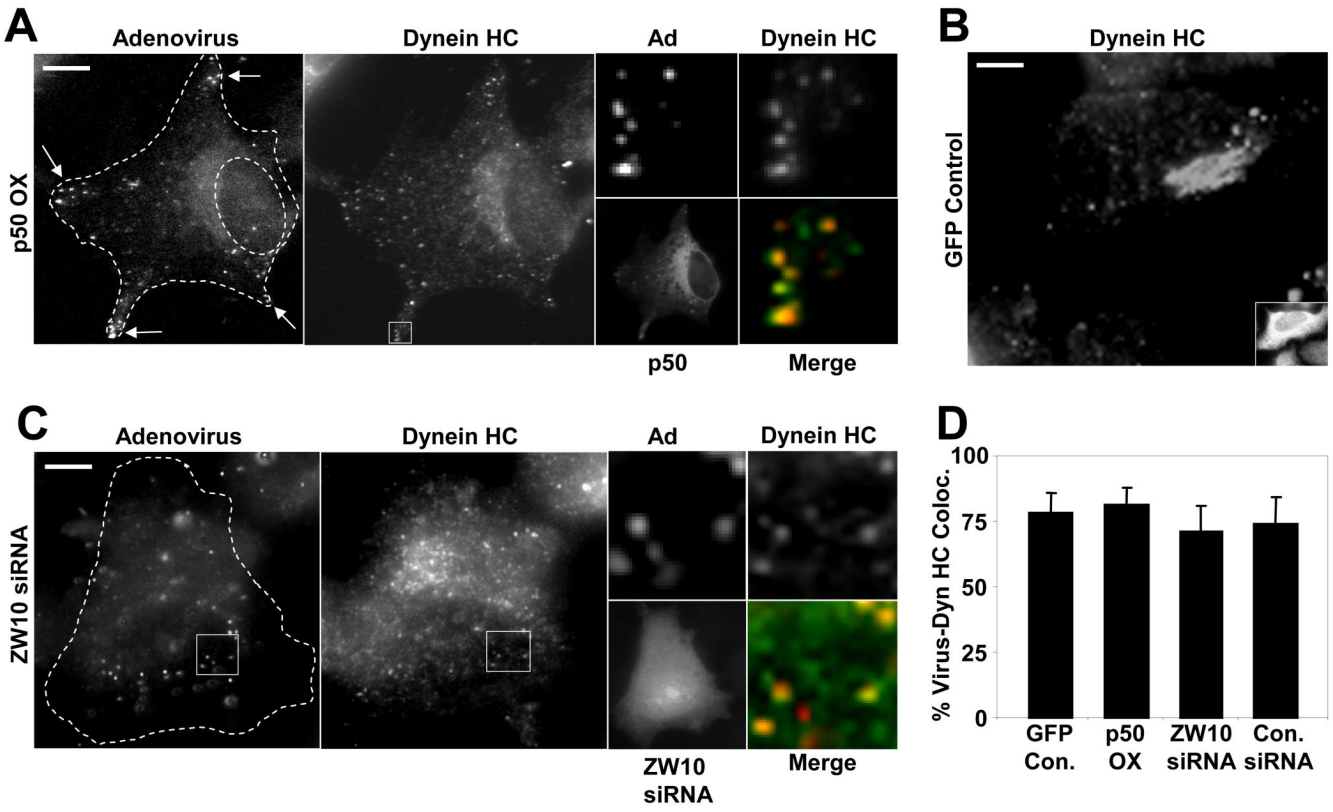

Figure 4. Dynein recruitment to adenovirus is independent of dynactin and ZW10

(**A**) HeLa cells were transfected with a cDNA encoding dynamitin-myc, infected at 24 hr with Cy3-Ad5 (red), and fixed and stained at 60 min p.i. for dynamitin and dynein HC (green). Dynein HC is still clearly detectable on virus particles (arrows) in whole cell image (boxed region is expanded at right), which are found largely in the cell periphery as a result of dynamitin overexpression. However, dynein HC localization to the Golgi apparatus was strongly inhibited *vs* control Golgi staining shown in panel **B**. (The weak juxtanuclear staining in the dynein HC panel (A) represents diffuse cytoplasmic staining in a thickened cell region, as further indicated by distribution of soluble myc-dynamitin.) (**C**) HeLa cells were transfected with ZW10 siRNA, infected with Cy3-Ad5 on day 3, fixed, and stained for dynein HC. Ad5 particles localized to the nucleus, consistent with a lack of function for ZW10 in Ad5 transport. Dynein HC staining at the Golgi apparatus was greatly reduced but was still clearly present on Ad5 particles (boxed region expanded at right). (**D**) Percent Ad5 particles colocalizing with dynein HC in dynamitin-overexpressing and ZW10 RNAi cells *vs* controls. All values are statistically insignificant compared to the control case ($P > 0.2$; t-test). Error bars represent SD. (Scale bars = 5 μm)

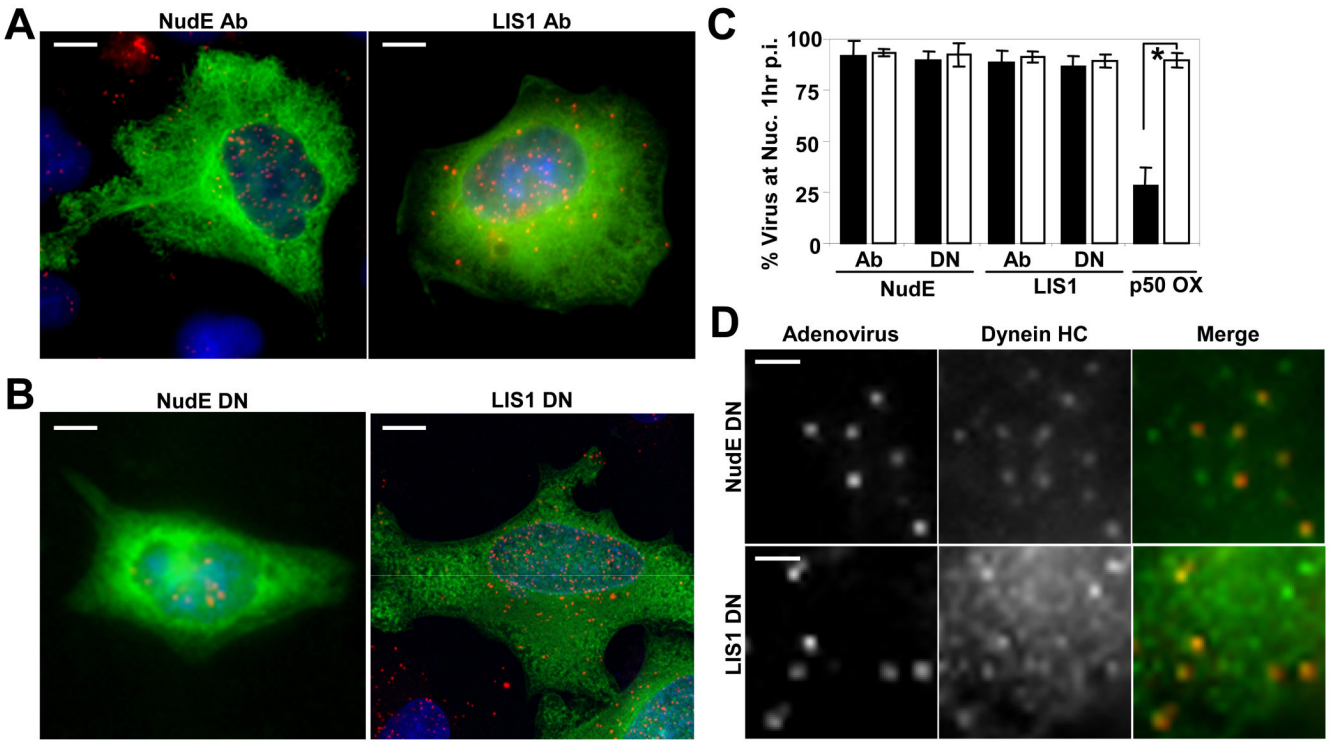

Figure 5. Ad5 transport and dynein recruitment are unaffected by NudE/NudEL and LIS1 inhibition

(**A**) A549 cells were microinjected with function-blocking NudE/NudEL or LIS1 antibodies (green), then infected with Cy3-Ad5 (red) before fixing and staining 60 min p.i. Nuclear accumulation of virus was observed in each case. (Scale bars = 5 μm) (**B**) HeLa cells were transfected with NudE or LIS1 dominant negative (DN) cDNA constructs (green). 24 hours after transfection, cells were infected with Cy3-Ad5 (red) and fixed 60 min p.i.. Again, clear nuclear accumulation of virus was observed. (Scale bars = 5 μm) (**C**) Percentage of cells exhibiting accumulation of Ad5 at the nucleus was determined for NudE/NudEL- and LIS1-inhibited cells (black bars). The effect of dynamitin (p50) overexpression on Ad5 nuclear accumulation is included for comparison. Open bars indicate results from control injected or transfected cells. Error bars represent SD. * indicates $P<0.01$; t-test. (**D**) Cy3-Ad5 (red) in HeLa cells overexpressing NudE or LIS1 DN cDNAs still colocalize with dynein HC (green). Panels show enlarged regions from a single cell. (Scale bars = 1 μm)

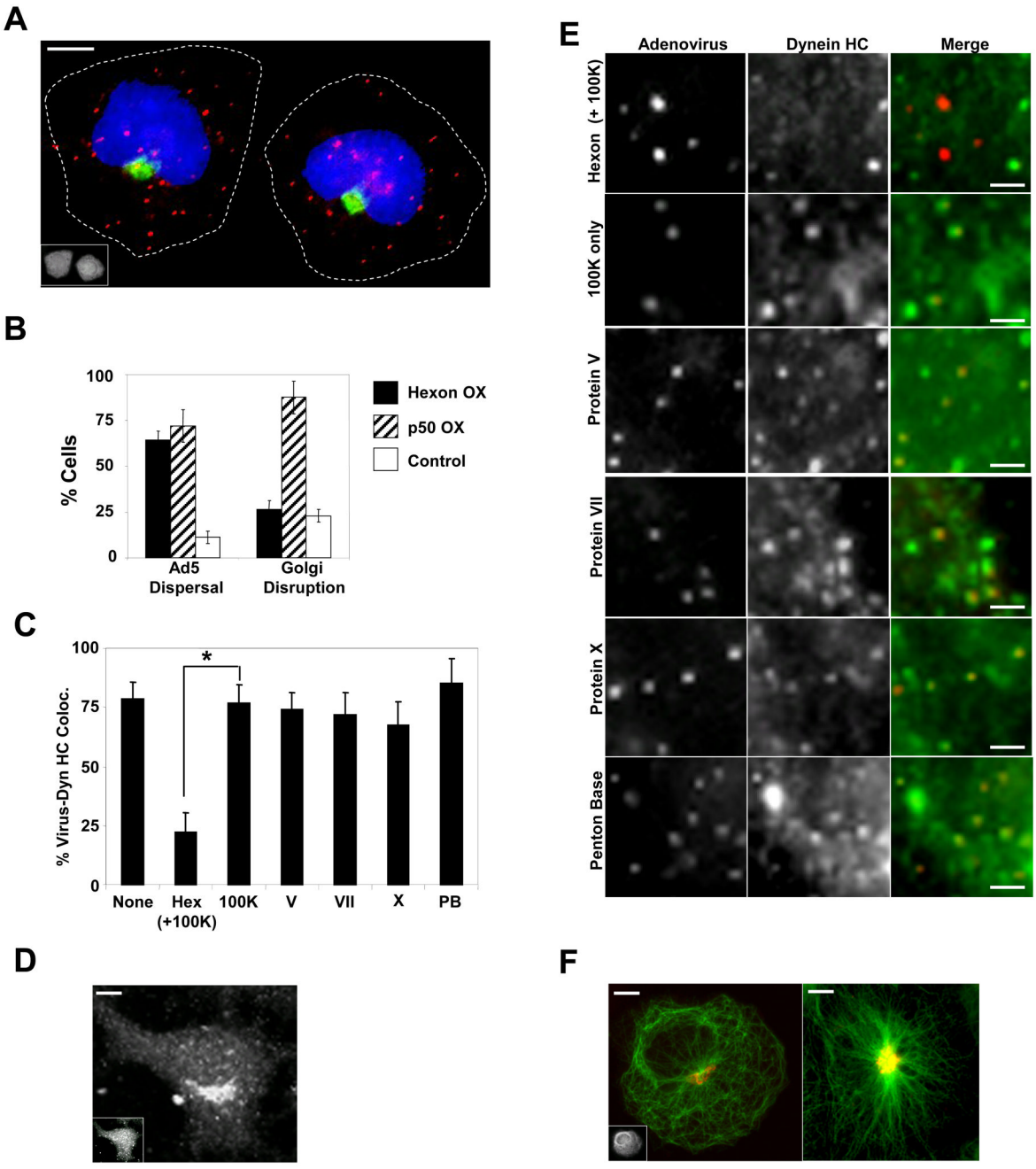

Figure 6. Hexon expression displaces dynein from incoming Ad5 and prevents viral accumulation at the nucleus

(**A**) HeLa cells expressing hexon (stained with anti-hexon monoclonal antibody, inset) show dispersed Ad5 particles (red) at 60 min p.i., but the centrosome-centered organization of the Golgi apparatus stained with anti-giantin (green) is unaffected. (scale bar: 5 μm) (**B**) Quantitative comparison of hexon and dynamitin effects on Ad5 distribution *vs* Golgi organization. Ad5 dispersal: Cells with below 70% of virions at nucleus at 60 min p.i.. Error bars represent +/− SD. (**C**) Percent of Ad5 particles positive for dynein HC +/− SD, determined as described for Fig 1. * indicates $P < 0.01$; t-test. (**D**) Dynein HC staining of the Golgi apparatus persists in hexon-expressing cell (inset). (scale bar: 5 μm) (**E**) HeLa cells transfected with

cDNAs encoding viral polypeptides were infected with Cy3-Ad5 (red) 48 hrs post-transfection, fixed at 60 min p.i. and stained for dynein HC (green). Panels show enlarged regions from individual cells. Dynein HC colocalization with adenovirus is disrupted by expression of hexon, but not of the other virus subunits. (scale bars: 1 μm) (**F**) Partial microtubule disorganization (anti-tubulin antibody, green) in a hexon-expressing cell (left), but with no apparent effect on Golgi organization (red), compared with the control (right). (scale bars: 5 μm)

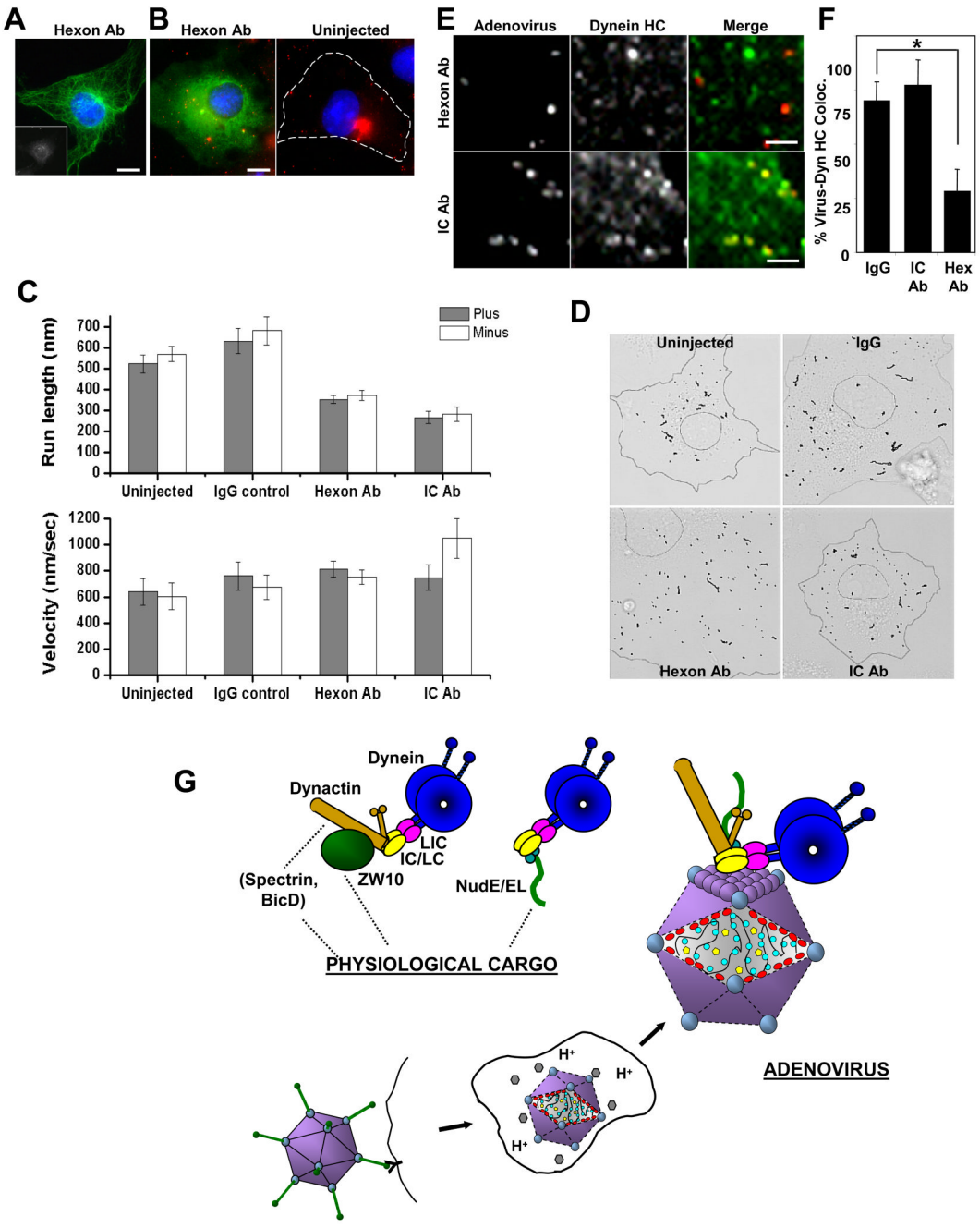

Figure 7. Anti-hexon antibody interferes with Ad5 transport

(**A**) COS-7 cell injected with monoclonal anti-hexon antibody (inset, stained with Cy5-conjugated secondary antibody) shows normal microtubule distribution as indicated by anti-tubulin immunostaining (green). (Scale bars: 5 μm) (**B**) COS-7 cells injected with anti-hexon antibody were infected with Alexa-Ad5, fixed 60 min p.i. and stained with Cy2-conjugated secondary antibody (green) and DAPI (blue). Ad5 particles were dispersed throughout the cytoplasm, whereas in control cells (right panel) the virus accumulated at the centrosome. (Scale bars: 5 μm) (**C**) Uninjected or antibody-injected cells were infected with Alexa-Ad5, and movies were acquired between 20 – 90 min p.i. for 1 min at 16 frames/sec. Anti-hexon and anti-dynein IC antibodies each significantly inhibited virus run length in both plus and

minus directions, but had minimal effect on velocity. Error bars represent +/− SEM. Motility data were extracted from analyzing 13 uninjected, 18 IgG injected, 27 anti-hex antibody injected, and 9 anti-dynein IC antibody injected cells. (**D**) Virus tracks from the duration of a representative 1 min movie were overlaid onto brightfield images to illustrate the effect of anti-hexon and anti-dynein IC on run length. Overall, shorter runs were observed in both antibody inhibited cases compared to the uninjected or IgG controls. (See also Supplemental Movies 1–4). (**E**) Antibody-injected, Alexa-Ad5 (red) infected cells were fixed 60 min p.i. and stained for dynein HC (green). Anti-hexon injection decreased colocalization of dynein HC with Ad5, whereas anti-dynein IC did not. (Scale bars: 1 μm) (**F**) Quantitative analysis of anti-hexon and anti-dynein antibody injection reveals loss of dynein HC from Alexa-Ad5 particles in anti-hexon, but not anti-IC, injected cells. * indicates $P < 0.01$; t-test. Error bars represent +/− SD. (**G**) Schematic representation of dynein association with adenovirus *vs* physiological cargo forms. Initial stages of infection are depicted, with dynein-binding occurring following release of the capsid from the early endosome. Dynein is shown binding directly to the capsid protein hexon (purple), as found in the current study. Diagram also depicts known Golgi and kinetochore dynein recruitment factors dynactin, ZW10, NudE, NudEL, Spectrin , and BicD. Dynactin is involved in both Golgi and kinetochore dynein recruitment, and NudE/NudEL in kinetochore as well as centrosome dynein recruitment (see text). These factors localize to adenovirus particles in the current study, but do not participate in dynein recruitment. Dynactin is, instead, found to regulate virus motility.